



# Photochemical modelling of the Barcelona area under weak pressure synoptic summer conditions

I. Toll and J. M. Baldasano

*Laboratory of Environmental Modelling, Department of Engineering Projects, Universitat Politècnica de Catalunya (UPC)*

*Avd. Diagonal 647, planta 10, 08028 Barceona, Spain*

*Email: baldasano@pe.upc.es*

## Abstract

The city of Barcelona and its surrounding area, located in the western Mediterranean basin, can reach high levels of  $O_3$  in summertime under weak pressure synoptic conditions. To study the origin of this photochemical pollution, the episode that took place between the 3 and 5 August 1990 was chosen. The main meteorological mesoscale flows that take place in the region, such as sea and land breeze, convection cells and topographic injections, were reproduced with the meteorological non-hydrostatic mesoscale model MEMO for 5 August 1990. Industrial and commercial activity on 5 August 1990 was very low because it was a Sunday in the summer holiday period. Therefore, the emissions inventory calculated for this day in an area of  $80 \times 80 \text{ km}^2$  around Barcelona showed that the main sources of VOC were traffic (51%) and vegetation (34%), while  $NO_x$  were mostly emitted by traffic (88%). Photochemical simulation with the MARS model has shown that the combination of mesoscale circulations and local emissions is crucial in the production of  $O_3$ . For instance,  $NO_x$  inland transport towards regions where biogenic VOC are emitted causes the formation of  $O_3$ , while topographic injections cause the formation of elevated  $O_3$  air layers. The synoptic wind, coming from the northeast in this case, also played an important role in advecting the air masses with local generated  $O_3$  away from their precursor emission sources. Evaluation of the model simulations is also performed and discussed by means of comparison of meteorological measurements in 9 surface stations and concentration measurements in 5 surface stations.

## 1 Introduction

Barcelona, a city located in the western Mediterranean basin in Spain, experienced an  $O_3$  episode from 3 to 5 August 1990 during a period of typical summertime meteorological conditions, that is, under weak pressure synoptic conditions. During the same period high  $O_3$  concentrations were registered in central and northern Europe (Ebel et al., 1995). The analysis of  $O_3$  concentration data in 5 measurement stations in the area of Barcelona showed that the maximum values were reached within the core of the urban area: Plaça Molina (125 ppb) and Hospitalet de Llobregat (170 ppb); but data in distant urban areas were not available (the air quality standard in the EU for  $O_3$  is 90 ppb in one hour).

In order to investigate the origin and formation of these high air pollution levels, simulations were carried out with the meteorological non-hydrostatic mesoscale model MEMO and the three-dimensional photochemical dispersion model MARS (Moussiopoulos, 1994). The simulation day chosen was 5 August, so that only industrial emissions from major factories would be included. VOC,  $NO_x$ , CO,  $SO_2$  and TSP emissions were calculated with the EIM-LEM model, a revised version of the one developed by Costa & Baldasano (1996), for anthropogenic sources. Biogenic VOC emissions were estimated by a methodology that takes local vegetation data into account (Gómez, 1998).

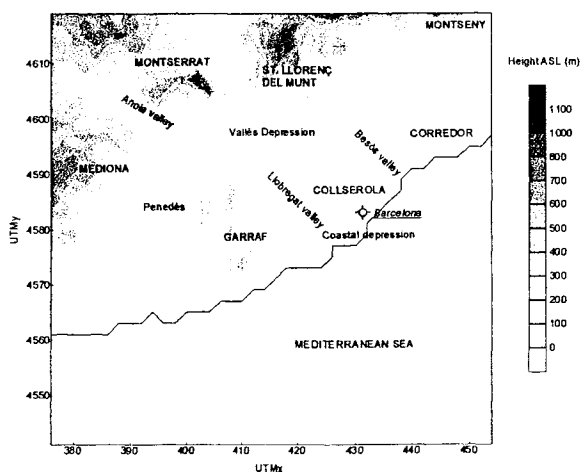


Figure 1: Topography of the geographical domain around Barcelona under study.

An 80x80 km<sup>2</sup> area centred around Barcelona (Figure 1) and including other densely populated towns such as Terrassa, Sabadell and Hospitalet was considered for this study (~ 4 million inhabitants). In addition, the terrain is complex and includes a coastal range, with the Garraf, Collserola and Corredor mountains, and a precoastal range with the Mediona, Montserrat, St. Llorenç del Munt and Montseny mountains. These areas are mainly covered by Mediterranean shrub and pine, oak and holm-oak forests. If crops are included, vegetation occupies 85% of the land considered in the domain studied.

The aim of this paper is to describe the main factors that contribute to photochemical production and transport of O<sub>3</sub>, during a daily cycle for this case study.

## 2 The characteristics and the input data of the model application

The meteorological and photochemical dispersion simulations were conducted in the same domain with a horizontal resolution of 2 km. The upper boundary was set to a height of 6000 m ASL and vertically the airshed was divided into 35 levels for the meteorological run, while the photochemical dispersion run was performed in the first 30 layers of those used for the meteorological one.

The initial conditions for the meteorological run, set at 21 LST (Local Standard Time=UTC+2) of the previous day, consisted of the temperature vertical profile measured in Nimes, while the geostrophic wind was derived from this sounding and the sounding acquired in Palma de Mallorca and set to 2 m/s from the northeast.

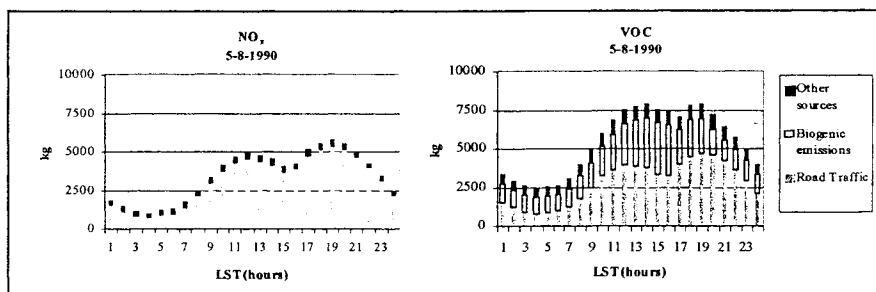


Figure 2: Hourly NO<sub>x</sub> and VOC emissions in the 80x80 km<sup>2</sup> domain on 5 August 1990.

Anthropogenic sources considered in the emissions inventory were: road traffic, industries, petrol stations, airport traffic, maritime traffic and port tanks, road

traffic being the major source on August 5. These emissions are concentrated in the urban areas, mainly Barcelona, and the roadways in the Besòs and Llobregat valleys, and in the Vallès depression. However, biogenic VOC emissions make up 34% of total emissions while road traffic emissions represent 51%. The highest biogenic VOC emissions took place at St Llorenç del Munt, Montserrat, Garraf and some forests located in the Vallès depression. The hourly distribution of the  $\text{NO}_x$  and VOC emissions are shown in Figure 2.

The photochemical dispersion model MARS was applied with the chemical mechanism EMEP (Simpson et al., 1993), which describes the tropospheric gas-phase chemistry with 66 species and 139 photochemical reactions. The VOC emissions were split into the 13 categories considered in the EMEP mechanism for each emitting source depending on its characteristics and based mainly on different bibliography sources.

A previous dispersion simulation with the same meteorological and emission data was used as initial conditions for the pollutant concentrations in the photochemical dispersion run. Inflow lateral boundary concentrations were derived from a simulation with the Lagrangian EMEP MSC-W model for Europe with an  $\text{O}_3$  concentration range between 14 and 63 ppb (Simpson, 1996).

### **3 Meteorological and photochemical dispersion modelling results**

The application of the meteorological non-hydrostatic mesoscale model MEMO in the area of study reproduced the land and sea breeze flows typically developing under weak summer synoptic pressure gradients, as well as the katabatic (downslope) and anabatic (upslope) winds on the main mountains in the domain.

During the early hours of the day, until 9 LST,  $\text{O}_3$  is depleted where NO is being emitted, mainly by road traffic both in the urban areas and at the main communication routes, as well as at a point source (glass manufacturer) located in south Barcelona (Zona Franca). Meanwhile, the land breeze transports this low  $\text{O}_3$  concentration air mass out over the Mediterranean Sea.

The sea breeze begins flowing inland between 10 and 12 LST and during the subsequent hours it is channelled inland through the Llobregat and Besòs valleys into the Vallès depression. This sea breeze causes the penetration of air masses loaded with  $\text{O}_3$  from the Mediterranean Sea which enters the domain through the lateral boundary conditions. The sea breeze flow is reinforced on the southern slopes of the coastal mountain range with the anabatic winds and does not penetrate beyond Collserola and Garraf until 16 LST.

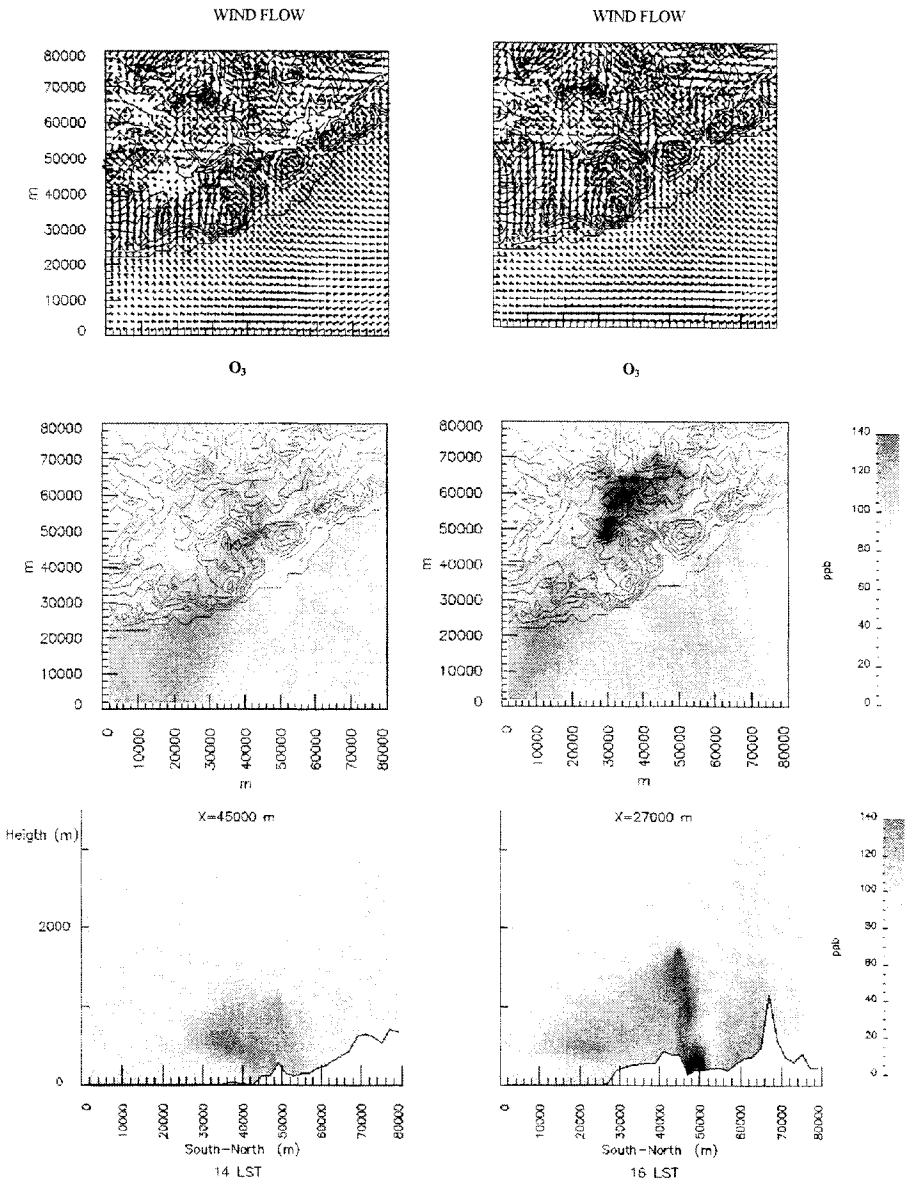


Figure 3: Wind flow and  $O_3$  concentrations in the 1st layer of the domain at 14 LST (left) and 16 LST (right). The vertical profiles of  $O_3$  concentration are at  $X=45000$  m and  $X=27000$  m respectively.

The photochemical formation of  $O_3$  begins around 11 LST in the planetary boundary layer (PBL), which at the same time is deepening due to the increasing intensity of solar radiation: between 13 and 14 LST the Garraf mountains and the Vallès depression are the areas with the highest levels of  $O_3$  (Figure 3). The higher concentrations of  $O_3$  in these areas are due to the fact that the sea breeze transports the  $NO_x$  emissions from the communication routes (road traffic) of the Llobregat valley towards them, while biogenic VOC are emitted at or near these geographical points.

Simultaneously, the above mentioned reinforcement of the sea breeze by the upslope winds in the coastal range, together with the increasing vertical mixing, drives ground air masses towards the upper layers of the PBL. This results in a layer of high  $O_3$  concentration at a height of around 600 m above the Llobregat valley (see Figure 3 for  $X=45000$  m). This upper nucleus of  $O_3$  will afterwards be advected towards the southwest by the geostrophic wind.

Between 15 and 16 LST the sea breeze flow in the Vallès depression gets stronger, transporting the  $NO_x$  emissions from the road traffic inland, which together with the higher biogenic VOC emissions in these hours results in an  $O_3$  concentration maximum. At the same time the vertical mixing and the convection cells formed over the Vallès transport these high  $O_3$  concentrations towards the upper air layers (see Figure 3 for  $X=27000$  m).

In the subsequent hours and until 19 LST photochemical activity is lower but the previously formed  $O_3$  is transported by the sea breeze and the anabatic winds towards the slopes of St. Llorenç del Munt and Montserrat. At Montserrat the high  $O_3$  concentration air masses undergo a topographic injection and are sent to heights between 1000 and 2000 m ASL.

From 20 LST until the end of the day the intensity of solar radiation decreases sharply, thus provoking a depletion of the  $O_3$  by  $NO$  in those places where the latter is emitted, as has been mentioned above in reference to the early hours of the day. The also decreasing vertical mixing decouples the ground  $O_3$  concentrations with those at higher air levels, which are advected towards the southwest (Penedès and Mediona range) by the geostrophic wind.

## 4 Evaluation of the simulations

The meteorological results were compared with 9 surface measurements within the modelling domain, the statistics for all of them being set out in Table 1. Figure 4 presents the model results and the measurements obtained at two stations as an example: Barcelona Airport (close to the sea) and St. Vicenç (14 km away from the coast in the Llobregat valley).

The temperature at both St. Vicenç and Barcelona Airport is underestimated by the model, but it has to be taken into account that the measurements were performed at 3 m AGL and the simulations at around 10 m AGL, and that the vertical temperature gradient can be pronounced near the ground. The statistics for all the stations in general show an underestimation of about 3°C and a negative bias for the same reason. The correlation coefficient is fairly good, and when performed for each meteorological station individually it was always above 0.8, except for the station of Tibidabo, because of its location near the top of the Collserola range in the middle of a forest, which is difficult to represent in its corresponding grid cell in the domain being considered.

The wind speed at both St. Vicenç and Barcelona Airport is well reproduced, the sea breeze arriving a little later at the first station. In general the statistics show a very slight underestimation of the wind speed, while the correlation coefficient is not very good. This is because: a) in some stations the simulated sea breeze and its maximum speed arrive a little later than the measured one, b) the modelled wind speed has a regular pattern while some measured wind speeds oscillate around a value, and c) the katabatic winds at two measurement stations located on mountain slopes are not well reproduced by the model, which underestimates them because of the grid resolution. The speed direction statistics have been separated into the sea (day) and land (night) breeze time periods, and only calculated for those with a physical sense. They show that the simulated wind directions are more northerly than those measured for the land breeze period, while during the sea breeze period the mean simulated wind was more easterly than the measured one.

Table 1: Statistics for the meteorological measurements and simulations.

	Temperature (9 stations)	Wind speed (8 stations)	Wind direction	
			Land breeze (6 stations)	Sea breeze (9 stations)
Mean observ.	28.1°C	2 m/s	330°	137°
Mean predict.	25.3°C	1.9 m/s	343°	129°
Bias	-3.6°C	-0.2 m/s	12°	-8.6°
Corr. coefficient	0.7	0.4		

As for the photochemical dispersion results, they were compared to the measurements in five surface stations, all located in urban areas. The statistics for all of them are shown in Table 2 while the hourly O<sub>3</sub> concentrations are plotted in Figure 5. In general the concentrations of NO, NO<sub>2</sub> and CO were overestimated and that of O<sub>3</sub> underestimated. The OP parameter is the % of simulated data higher than the observed data for the same time, and shows that in spite of the general model overestimation, 47% of the measured concentrations were lower than the simulated ones for NO. This happened mainly because the NO is overpredicted at the end of the day at the Plaça Molina and Hospitalet

stations, while the  $O_3$  disappears too quickly. This could be explained by excessively rapid depletion in the model, but also by NO overestimation in the emissions and/or a lack of reproduction of the microscale meteorological processes in these urban locations during the night; this is plausible because the CO, a low reactive species, was also overestimated at these times and locations.

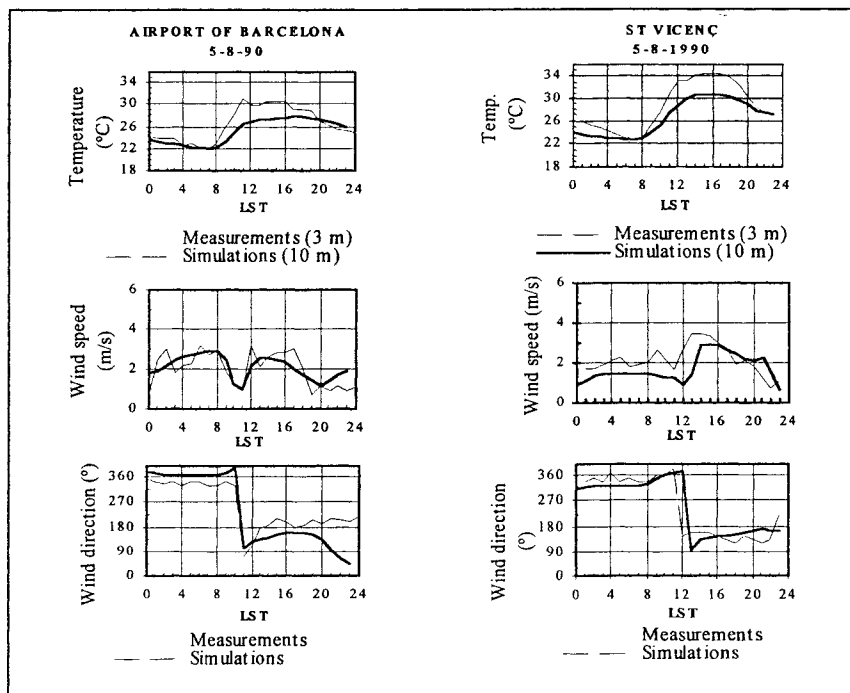


Figure 4: Comparison of the measured and simulated temperature, wind speed and direction at St. Vicenç and Barcelona Airport.

Table 2: Statistics for the photochemical dispersion measurements and simulations.

	NO (4 stations)	NO <sub>2</sub> (4 stations)	CO (5 stations)	O <sub>3</sub> (4 stations)
Mean observ.	17.96 ppb	26.32 ppb	722.33 ppb	46.95 ppb
Mean predictions	19.63 ppb	35.32 ppb	842.03 ppb	31.20 ppb
Bias	2.66	8.49	119.70	-15.75
OP	0.47	0.60	0.62	0.25

$O_3$  concentrations were closely reproduced at Badalona (close to the sea) and Montcada (about 7 km from the coast), but underestimated at Plaça Molina and



Hospitalet, which are located within the urban core. The concentration levels at these stations are also quite sensitive to the background concentrations of the air masses over the Mediterranean Sea, since these are being transported towards them by the sea breeze, and are introduced as lateral boundary conditions. Concerning the high  $O_3$  concentrations simulated further from the city of Barcelona in the Vallès depression, no measurement data were available to evaluate them in the upper air layers. Other authors have reported the presence of upper air polluted masses in Spain (Millán et al., 1997) and in the Barcelona area (Soriano et al., 1999), but further research needs to be carried out in this region.

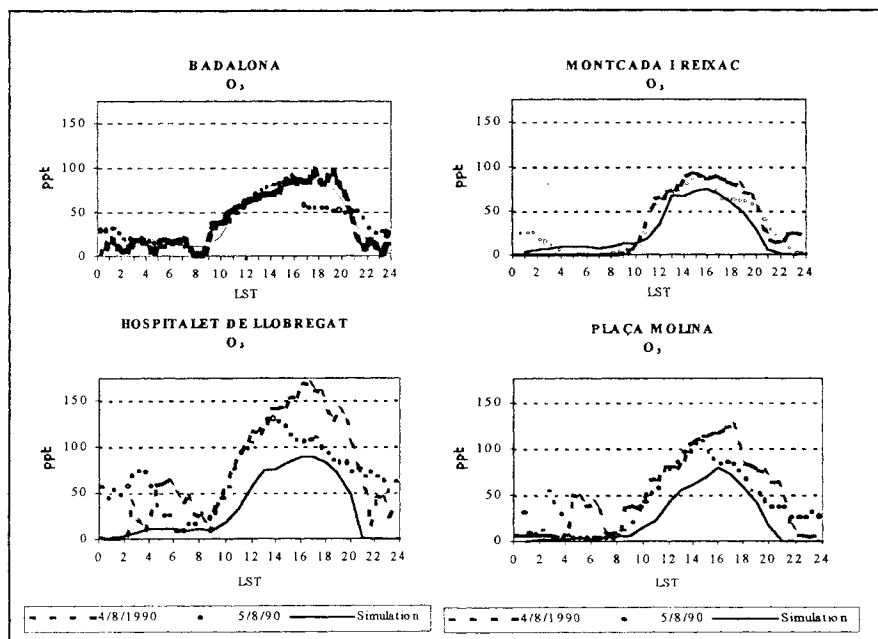


Figure 5: Comparison of the measured and simulated  $O_3$  concentrations at the four surface stations where it was measured on 5 August 1990.

## 5 Conclusions

Simulations carried out with the meteorological non-hydrostatic mesoscale model (MEMO), the emissions inventory model (EIM-LEM) and a photochemical dispersion model (MARS) of an  $O_3$  episode under weak pressure synoptic summer conditions in the Barcelona area indicate that high  $O_3$  concentrations might occur in locations where anthropogenically emitted  $NO_x$  and biogenic VOC meet. In this case study this happens between 15 and 16 LST in the Vallès depression because of: a) higher biogenic VOC emissions and  $NO_x$



emissions from the nearby roadways b) advection of these  $\text{NO}_x$  towards the vegetation units by the sea breeze and c) high photochemical activity. This  $\text{O}_3$  is also injected into the upper air layers, both in the coastal range (Garraf and Collserola) and in the precoastal range (mainly near Montserrat). However, part of the  $\text{O}_3$  air concentrations found inland are due to the sea breeze introducing the domain's lateral boundary concentrations. The simulation results, both meteorological and for photochemical dispersion, were compared with surface measurement stations, and proved to be fairly close; but further validation with other case studies needs to be done with rural measurements and vertical soundings data.

## References

- Costa, M. & Baldasano, J.M. (1996). Development of a Source Emission Model for Atmospheric Pollutants of the Barcelona area. *Atmospheric Environment*, **30A**, 2, pp. 309-318.
- Ebel, A., Elbern, H., Hass, H., Jakobs, H.J., Memmesheimer, M. & Bock, H.J. (1995). Meteorological effects on air pollutant variability on regional scales., *Air Pollution III, Vol. 4*, eds. A. Ebel & N. Moussiopoulos, Computational Mechanics Publications, Southampton, pp. 1-6.
- Gómez, O. (1998). *Estimación de las emisiones de COV biogénicos de origen terrestre para Cataluña*. PhD thesis, Universitat Politècnica de Catalunya, Barcelona.
- Millán, M., Salvador, R., Mantilla, E. & Kallos G. (1997). Photooxidant dynamics in the Mediterranean basin in summer: Results from European research projects. *Journal of Geophysical Research*, **102**, D7, pp. 8811-8823.
- Moussiopoulos, N. (1994). *The EUMAC Zooming Model. Model structure and applications*, ed. N. Moussiopoulos, EUROTRAC, Garmisch-Partenkirchen, pp. 1-266.
- Simpson, D. et al. (1993). *Updating the chemical scheme for the EMEP MSC-W oxidant model: current status*, EMEP MSC-W Note 2/93, Oslo.
- Simpson, D. (1996). *Personal communication*.
- Soriano, C., Baldasano, J.M., Buttler, W.T. & Moore K.R. (1999). Circulatory Patterns of Air Pollutants within Barcelona Air Basin in a Summertime Situation: Lidar and Numerical Approaches. *Journal of Geophysical Research* (at review stage).